



Published in final edited form as:

J Org Chem. 2015 August 7; 80(15): 7403–7411. doi:10.1021/acs.joc.5b01023.

Direct Observation of Intermediates Involved in the Interruption of the Bischler–Napieralski Reaction

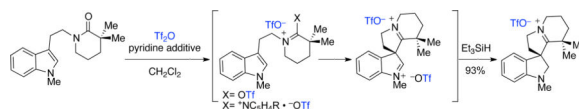
Kolby L. White, Marius Mewald, and Mohammad Movassaghi*

Department of Chemistry, Massachusetts Institute of Technology, Cambridge, Massachusetts 02139, United States

Abstract

The first mechanistic investigation of electrophilic amide activation of α,α -disubstituted tertiary lactams and the direct observation of key intermediates by in situ FTIR, ^1H , ^{13}C , and ^{19}F NMR in our interrupted Bischler–Napieralski based synthetic strategy to the aspidosperma alkaloids, including a complex tetracyclic diiminium ion, is discussed. The reactivity of a wide range of pyridines with trifluoromethanesulfonic anhydride was systematically examined, and characteristic IR absorption bands for the corresponding *N*-trifluoromethanesulfonylated pyridinium trifluoromethanesulfonates were assigned. The reversible formation of diiminium ether intermediates was studied, providing insight into divergent mechanistic pathways as a function of the steric environment of the amide substrate and stoichiometry of reagents. Importantly, when considering base additives during electrophilic amide activation, more hindered α -quaternary tertiary lactams require the use of non-nucleophilic pyridine additives in order to avoid deactivation via a competing desulfonylation reaction. The isolation and full characterization of a tetracyclic iminium trifluoromethanesulfonate provided additional correlation between in situ characterization of sensitive intermediates and isolable compounds involved in this synthetic transformation.

Graphical abstract



Introduction

Trifluoromethanesulfonic anhydride (Tf_2O) has been employed as an electrophilic reagent for activation of a wide range of functional groups.¹ These transformations often include condensation reactions that are sensitive to the base additive or presence of Lewis basic

*Corresponding Author. movassag@mit.edu.

ASSOCIATED CONTENT

Supporting Information Copies of ^1H and ^{13}C NMR spectra of all compounds described in the experimental section. This material is available free of charge via the Internet at <http://pubs.acs.org>

Notes

The authors declare no competing financial interest.

functional group. We have found the Tf₂O–2-chloropyridine reagent combination, first reported by Myers for the synthesis of a key vinyl trifluoromethanesulfonate in their total synthesis of (+)-dynemicin A² and later by Gin for dehydrative glycosylation chemistry,³ to be particularly effective for electrophilic amide activation leading to an array of versatile condensation reactions that include syntheses of substituted pyridines,⁴ pyrimidines,^{5,6} alkynyl imines,⁷ isoquinolines and β-carbolines.⁸ We also first reported the use of the Tf₂O–2-fluoropyridine reagent combination for direct dehydrative *N*-pyridinylation of amides.⁹ Contributions from other research groups¹⁰ have resulted in exciting transformations that include chemoselective reduction of amides,¹¹ reductive alkylation of amides and lactams,¹² α-arylation of amides,¹³ and syntheses of ketones and ketimines.^{14,15} Recently, we have applied this amide activation chemistry to access spirocyclic indolines via the interruption of the Bischler–Napieralski reaction,¹⁶ and applied this strategy to the total synthesis of various members of the aspidosperma alkaloids.¹⁷ While new applications of this amide activation chemistry continue to offer unique and versatile synthetic transformations, the paucity of detailed studies concerning the identity and reactivity of crucial intermediates prompted our investigation of sensitive and electrophilic compounds involved in this chemistry. Herein, we report the first direct monitoring of the electrophilic amide activation of tertiary lactams and the subsequent observation of the resulting *O*-trifluoromethanesulfonyloxyiminium ions, mono- and diiminium spiroindolines, and diiminium ethers through the use of in situ reaction monitoring techniques.

Amide activation with Tf₂O occurs through the attack of the amide oxygen onto the electrophilic sulfur, followed by expulsion of a trifluoromethanesulfonate ion (Scheme 1).^{5a,18} The resulting *O*-trifluoromethanesulfonyloxyiminium trifluoromethanesulfonate **3** can further react with pyridine additive **2** to form 1-pyridyliminium bistrifluoromethanesulfonate **4**. However, some pyridines can add to Tf₂O in competition with the amide substrate, resulting in the formation of *N*-(trifluoromethylsulfonyl)pyridinium trifluoromethanesulfonate **5** that may transfer the sulfonyl to the amide, providing an alternative pathway to **3**. In the case of tertiary amide substrates, the corresponding activated iminium ions are particularly reactive and in situ monitoring techniques are necessary to study persistent intermediates. As an outgrowth of our continuing interest in probing the mechanism of electrophilic amide activation,^{5a,9} and informed by the pioneering studies of Charette¹⁸ in addition to the recent incisive investigation by Maulide,¹³ we embarked on a detailed study involving tertiary lactams that was designed to interrogate the effect of different pyridine additives on the rate of amide activation, the ensuing spirocyclization when applicable,^{16,17} as well as their influence on the chemical stability of electrophilic intermediates.^{19,20}

Results and Discussion

Electrophilic Activation of Tertiary Lactams in the Absence of Pyridine Bases

We began our mechanistic study of the interruption of the Bischler–Napieralski reaction with the systematic study of the electrophilic activation of amides in the absence or the presence of pyridine additives. In order to develop ideal conditions for spirocyclization, it was necessary to first investigate the electrophilic activation of simple tertiary lactams. This

allowed for the identification of the lowest temperature for efficient tertiary lactam activation and a reference for the influence of base additives. We began our studies with tertiary, six-membered ring lactams **1a** and **1b** (Scheme 2A) because they possess important characteristics of the lactam substrates we have utilized in our total synthesis efforts,¹⁷ but lack functional groups that would obscure the region of interest in the IR spectra. Lactams **1a** (1625 cm⁻¹) and **1b** (1621 cm⁻¹) both react with Tf₂O at -78 °C to form the corresponding *O*-trifluoromethanesulfonyloxyiminium trifluoromethanesulfonates **3a** (1692 cm⁻¹) and **3b** (1664 cm⁻¹), respectively.²¹ This can be directly monitored by IR through the rapid disappearance of the carbonyl absorption band at 1625 cm⁻¹ and 1621 cm⁻¹, respectively, and simultaneous formation of what we postulate to be the iminium ion absorption bands of the *O*-trifluoromethanesulfonyloxyiminium trifluoromethanesulfonate **3a** and **3b** at 1692 cm⁻¹ and 1664 cm⁻¹, respectively (Scheme 2B). The formation of **3a** and **3b** was also monitored by ¹H, ¹³C and ¹⁹F NMR. In each case two key ¹⁹F NMR resonances were observed that support the formation of **3a** and **3b**,²² one corresponding to the trifluoromethanesulfonate anion (-79.4 and -79.7 ppm, respectively) and another corresponding to the fluorine resonance of the *O*-trifluoromethanesulfonyloxyiminium at -72.3 ppm and -71.1 ppm for **3a** and **3b**, respectively.¹⁸

During in situ IR monitoring of the activation of lactam **1a**, we noticed the transient formation of an absorption band at 1675 cm⁻¹ in the IR spectrum (Scheme 2C). To further probe the identity of this intermediate, activation of **1a** using 0.5 equivalents of Tf₂O was examined. The immediate product detected by IR is the expected *O*-trifluoromethanesulfonyloxyiminium trifluoromethanesulfonate **3a**. However, even at -78 °C, an absorption band at 1675 cm⁻¹ appears and grows in intensity as the absorption bands at 1625 cm⁻¹ (**1a**) and 1692 cm⁻¹ (**3a**) disappear (Scheme 2C). We postulate the absorption band at 1675 cm⁻¹ to correspond to formation of diiminium ether **6a** (1675 cm⁻¹).²² This hypothesis was further supported through ¹H and ¹⁹F NMR analysis, as the use of 0.5 equivalents of Tf₂O resulted in the formation of a single species with distinct chemical shifts. Most importantly, the ¹⁹F NMR no longer contains a resonance corresponding to the *O*-trifluoromethylsulfonyl group present in **3a**, consistent with diiminium ether formation.^{22,23} The attack of amides onto *O*-trifluoromethanesulfonyloxyiminium ions has been documented,^{22,23} but this is the first instance of tertiary lactams forming these highly reactive dication intermediates. Through in situ IR monitoring we also observe the formation of diiminium ether **6b** (1644 cm⁻¹), which requires warming to 23 °C due to the increased steric environment of *O*-trifluoromethanesulfonyloxyiminium ion **3b**.

Based on our initial findings with the synthesis of diiminium ethers **6a** and **6b** from lactams **1a** and **1b** (Scheme 2), we conducted additional experiments focused on the formation of mixed diiminium ether **7** (Scheme 3, 1675 cm⁻¹, 1644 cm⁻¹). Through these experiments we hoped to gain more information on the difference in reactivity between *O*-trifluoromethanesulfonyloxyiminium trifluoromethanesulfonates **3a** and **3b**. In order to synthesize diiminium ether **7**, lactam **1b** was added to a solution of *O*-trifluoromethanesulfonyloxyiminium trifluoromethanesulfonate **3a** (Scheme 3, step b). Two absorption bands at 1675 cm⁻¹ and 1644 cm⁻¹ emerged in the IR spectrum and are consistent with the formation of the diiminium ether **7**. While the sensitivity and reactivity

of this compound prevent its isolation, our observations support the formation of mixed diiminium ether **7** and not a mixture of diiminium ethers **6a** and **6b**.²⁴ Interestingly, the reaction profile of the addition of lactam **1a** to *O*-trifluoromethanesulfonyloxyiminium trifluoromethanesulfonate **3b** is more complex and further emphasizes the difference in reactivity between lactam **1a** and **1b** (Scheme 3, step c). First, partial transfer of the trifluoromethylsulfonyl group from *O*-sulfonyliminium sulfonate **3b** to lactam **1a**, forming *O*-sulfonyliminium sulfonate **3a** occurs in less than 30 seconds at $-78\text{ }^{\circ}\text{C}$ which was supported by an absorption band at 1692 cm^{-1} . This was followed by the formation of diiminium ether **6a** and a small amount of mixed diiminium ether **7**. Both *O*-trifluoromethanesulfonyloxyiminium trifluoromethanesulfonate **3b** and lactam **1b** also remain, and after 30 minutes at $23\text{ }^{\circ}\text{C}$, the major product was the mixed diiminium ether **7** (Scheme 3, step d). This suggests that the system is dynamic, and that the diiminium ether is a more stable intermediate than the *O*-trifluoromethanesulfonyloxyiminium trifluoromethanesulfonates **3a** and **3b**. This interesting result further demonstrates the marked difference in reactivity between unhindered lactam **1a** and α -quaternary lactam **1b**. This observation is also consistent with *O*-trifluoromethanesulfonyloxyiminium trifluoromethanesulfonate **3b** acting as a sulfonylating reagent instead of reacting at carbon due to the steric pressure at the α -position. While this type of iminium ethers may be formed competitively as undesired by-products during amide activation, the observed difference in reactivity between lactam **1a** and **1b** highlights the unique challenge associated with hindered lactams as substrates in this chemistry compared to previously studied systems^{13,18} due to potential competitive desulfonylation.

Electrophilic Activation of Tertiary Lactams in the Presence of Pyridine Bases

By examining a range of pyridine additives with electron-withdrawing and electron-donating substituents, we sought to understand how these substituents influence the reactivity of pyridines with Tf_2O (Table 1). Alkyl amines and alkyl substituted pyridines were not examined in this study based on their documented oxidation with Tf_2O .^{1b,25} By first establishing the reactivity of each substituted pyridine with Tf_2O , we also planned to determine the IR absorption bands for the corresponding *N*-(trifluoromethylsulfonyl)pyridinium trifluoromethanesulfonates (Table 1), allowing for an informed analysis during in situ IR monitoring of lactam activation with various pyridine additives. When pyridine is combined with Tf_2O in dichloromethane, the corresponding *N*-(trifluoromethylsulfonyl)pyridinium trifluoromethanesulfonate **5** (R=H) is formed rapidly (Table 1, entry 1).^{18,26} Interestingly, we had previously observed that 2-chloropyridine does not react with Tf_2O in dichloromethane, even after extended reaction time (Table 1, entry 2).^{5a} We found that 2-fluoropyridine and other electron deficient pyridines were slow to undergo *N*-sulfonylation at $-78\text{ }^{\circ}\text{C}$. For example, 2-fluoropyridine (Table 1, entry 3) required warming to $23\text{ }^{\circ}\text{C}$ before significant (ca. 1/3) conversion to the corresponding *N*-(trifluoromethylsulfonyl)pyridinium trifluoromethanesulfonate. In this respect, the reagent combination of Tf_2O -2-chloropyridine is unique in its resistance to undergo *N*-sulfonylation under the reaction conditions.^{5a} While electron-deficient pyridines react slowly with Tf_2O to give the corresponding *N*-sulfonyl pyridinium ion **5** (Table 1, entries 2–9), they do not interfere with amide activation due to the rapid rate of the reaction between Tf_2O and lactams at $-78\text{ }^{\circ}\text{C}$. However, the electron-rich pyridines we investigated react rapidly with

Tf₂O, even at -78 °C, to provide *N*-sulfonyl pyridinium ion **5** (Table 1, entries 10–11). A combination of steric hindrance around the pyridine nitrogen and the influence of an electron-withdrawing substituent may be best illustrated in the case of 2-chloropyridine, rendering it unique amongst the additives examined in Table 1. The evaluation of the rate of reaction of pyridine derivatives with Tf₂O is informative in our selection of base additives that minimize competing undesired deactivation when using hindered amide substrates as discussed below.

We then investigated the interaction of *O*-trifluoromethanesulfonyloxyiminium trifluoromethanesulfonates with different pyridine additives.²⁷ In situ IR analysis allowed for monitoring of the formation of 1-pyridyliminium bistrifluoromethanesulfonates **4a** and **4b** from the sulfonyliminium ions **3a** and **3b**, respectively, by treatment with different pyridine additives (Table 2A). Interestingly, activation of lactam **1a** occurs in the presence of electron-rich pyridines that react rapidly with Tf₂O at -78 °C (Table 2A, entry 3), as well as in the presence of less nucleophilic electron-deficient pyridines (Table 2A, entry 1), demonstrating its enhanced nucleophilicity relative to α,α -disubstituted lactam **1b** (vide supra). However, our primary interest was the examination of more sterically hindered lactams, consistent with substrates required for our interrupted Bischler–Napieralski based synthetic strategy to the aspidosperma alkaloids, similar to α,α -disubstituted lactam **1b**.

In the more critical case of lactam **1b**, we discovered that electron-rich pyridine additives completely shut down the lactam activation pathway by intercepting the highly electrophilic Tf₂O before nucleophilic attack of the lactam **1b**. When electron-deficient pyridines are used as additives, amide activation of lactam **1b** with Tf₂O proceeds smoothly followed by addition of the pyridine additives onto sulfonyliminium ion **3b** to afford the corresponding 1-pyridyliminium ion **4b** (Table 2, entries 4–8). The key IR absorption bands for 1-pyridyliminium ions **4b** are consistent with the observed formation of a new set of IR absorption bands, as a function of the pyridine additive, with concomitant disappearance of the IR absorption band for sulfonyliminium ion **3b**. A representative example is illustrated for the conversion of lactam **1b** to the corresponding 1-pyridyliminium ion **4b** (R" = 4-CN, 1633 cm⁻¹) upon activation of lactam **1b** with Tf₂O in the presence of 4-cyanopyridine (Table 2B). Furthermore, we conducted NMR experiments in tandem with our IR study using 3-chloropyridine (Table 2, entry 5), and we observed the formation of a new and distinct species upon treatment of sulfonyliminium ion **3b** with 3-chloropyridine. Similar to NMR monitoring experiments concerning the formation of diiminium ethers (vide supra), only the ¹⁹F NMR resonance corresponding to the trifluoromethanesulfonate anion was observed after treatment of sulfonyliminium ion **3b** with 3-chloropyridine. This observation is consistent with the expulsion of a trifluoromethanesulfonate ion from sulfonyliminium ion **3b**, and supports the hypothesis that the appearance of new IR absorption bands seen upon treatment of sulfonyliminium ion **3b** with pyridine derivatives, accounts for the formation of 1-pyridyliminium ion **4b**. As anticipated, the rates of amide activation and subsequent pyridine addition were strongly dependent on the substituents on the pyridine additive. Pyridines with electron-withdrawing substituents at the 2-position undergo slower addition to the *O*-trifluoromethanesulfonyloxyiminium ion, but do not hinder the initial activation of the lactam (Table 2A, entries 3–4). Pyridines with electron-withdrawing substituents at the

3- and 4-position formed the corresponding 1-pyridyliminium ion **4b** in less than 2 minutes at $-78\text{ }^{\circ}\text{C}$ (Table 2, entries 5–7).

As discussed above, each pyridine additive explored underwent *N*-sulfonylation using the conditions examined (Table 1) except for 2-chloropyridine. Continuing our efforts towards understanding the chemistry of *O*-trifluoromethanesulfonyliminium trifluoromethanesulfonates, we were interested in determining which *N*-(trifluoromethylsulfonyl)pyridinium trifluoromethanesulfonates **5** can act as electrophilic amide activation reagents. Representative *N*-(trifluoromethylsulfonyl)pyridinium trifluoromethanesulfonates were synthesized, and after their complete formation was observed by in situ IR analysis, lactam **1a** or **1b** was introduced to the reaction mixture. By comparing the reaction profile to that in which Tf_2O was added to the pyridine–lactam mixture, it was possible to determine the dominant activation path in each case examined (Table 2, entries 2, 4, 6, 7). In the case of 2-chloropyridine, formation of the *N*-(trifluoromethylsulfonyl)pyridinium trifluoromethanesulfonate does not occur, which results in direct attack onto Tf_2O by either lactams **1a** or **1b**. We postulate that this is a major contributing factor to the broad utility of the Tf_2O –2-chloropyridine reagent combination. All *N*-(trifluoromethylsulfonyl)pyridinium trifluoromethanesulfonate derivatives prepared from mildly nucleophilic pyridines (Table 2A) led to activation of the lactams **1a** or **1b**, albeit at a slower rate relative to standard conditions involving addition of Tf_2O to the pyridine–lactam mixture. This diminished rate of electrophilic activation observed when premixing the pyridine additive with Tf_2O is consistent with the dominant pathway for lactam activation involving direct attack onto Tf_2O by the lactam.

In order to examine the inhibitory effect of electron-rich pyridines on the activation of sterically hindered lactam **1b**, we monitored the addition of pyridine to sulfonyliminium ion **3b** (Scheme 4A). Treatment of lactam **1b** with Tf_2O (1.2 equiv) in dichloromethane at $-78\text{ }^{\circ}\text{C}$ followed by warming to $23\text{ }^{\circ}\text{C}$ led to clean formation of sulfonyliminium ion **3b** (Scheme 4B). After cooling the reaction mixture to $-78\text{ }^{\circ}\text{C}$ and introduction of pyridine (2 equiv), immediate reversion to starting lactam **1b** and formation of *N*-(trifluoromethylsulfonyl)pyridinium trifluoromethanesulfonate **5** ($\text{R}=\text{H}$, 1687 cm^{-1} , 1629 cm^{-1}) is observed by both in situ NMR and IR monitoring experiments instead of the anticipated formation of 1-pyridyliminium ion **4b** ($\text{R}=\text{H}$). Importantly, this observation highlights the influence of the steric crowding around the sulfonyliminium ion **3b**, which results in nucleophilic attack by pyridine at the sulfur rather than the carbon of the trifluoromethylsulfonyliminium functional group. Pyridinium **5** ($\text{R}=\text{H}$) is not sufficiently electrophilic to effectively sulfonylate α,α -disubstituted lactam **1b**, thus leading to deactivation and regeneration of lactam **1b** (Scheme 4B). For comparison, electron-deficient pyridines (Table 2) allow for activation of sterically hindered lactams under similar conditions because the corresponding *N*-(trifluoromethylsulfonyl)pyridinium trifluoromethanesulfonate is formed at a slower rate and serves as a better sulfonylating reagent. This shifts the equilibrium more towards activated lactam **3b** and enables the formation of 1-pyridyliminium trifluoromethanesulfonate **4b** (Table 2).

In Situ Study of the Interruption of the Bischler–Napieralski Reaction

Using the information gained above from examining Tf₂O-mediated lactam activation, we expanded our in situ reaction monitoring studies to indole lactam **8** (Scheme 5) enabling us to monitor the tandem activation-spirocyclization to form spirodiiminium ion (±)-**11**. In these experiments, we aimed to determine the reaction rate, the influence of the pyridine additives on the spirocyclization event, and to identify key intermediates while also evaluating their thermal stability.

Treatment of lactam **8** with Tf₂O in dichloromethane at –78 °C in the absence of any pyridine additive led to the formation of *O*-trifluoromethanesulfonyloxyiminium trifluoromethanesulfonate **9** at –78 °C in less than one minute (Scheme 5A). This transformation can be monitored by IR through the disappearance of the lactam amide **8** absorption band at 1621 cm^{–1}, and simultaneous formation of an absorption band at 1659 cm^{–1} corresponding to iminium ion **9** (Scheme 5B). Additionally, the formation of iminium ion **9** was consistent with the emergence of a distinct set of new resonances as observed by monitoring the reaction progress by in situ ¹H NMR analysis. Notably, the ¹³C and ¹⁹F NMR analysis of the reaction mixture is consistent with our observations concerning the formation of *O*-trifluoromethanesulfonyloxyiminium trifluoromethanesulfonate **3**, in that we see a clear ¹³C NMR resonance at 174.6 ppm corresponding to the C13 of the iminium ion and two fluorine resonances at –79.9 ppm and –71.4 ppm corresponding to the trifluoromethanesulfonate anion and *O*-trifluoromethanesulfonyloxyiminium, respectively (vide supra). Upon warming to 0 °C, the IR absorption band at 1659 cm^{–1} slowly broadens before eventually forming two absorption bands at 1664 cm^{–1} and 1644 cm^{–1}, which correspond to diiminium ion (±)-**11** (Scheme 5). By monitoring of the reaction mixture with variable temperature NMR while slow warming from –78 °C, we were able to see trace formation of diiminium ion (±)-**11** at –40 °C (<5% after 30 minutes at –40 °C), and observed full conversion after 10 minutes at 0 °C (Figure 1). Key ¹H NMR resonances consistent with conversion of iminium ion **9** to diiminium ion (±)-**11** include the downfield shift of C2-H resonance from 7.03 ppm to 10.02 ppm and the downfield shift of N-Me resonance from 3.72 ppm to 4.33 ppm. Additionally, while the ¹³C and ¹⁹F resonances at 174.6 ppm and –71.4 ppm, respectively, corresponding to the *O*-trifluoromethanesulfonyloxyiminium ion **9** disappear, two carbon resonances at 176.2 ppm and 187.9 ppm corresponding to the C2- and C19-iminium ions of tetracycle (±)-**11**, respectively, appear, and the intensity of the trifluoromethanesulfonate anion resonance in the ¹⁹F NMR spectra at –79.9 ppm increases.

In the presence of pyridine additives, the absorption band for *O*-trifluoromethanesulfonyloxyiminium trifluoromethanesulfonate **9** is transient and absorption bands corresponding to the formation of 1-pyridyliminium ion **10** are observed by both in situ IR and NMR. Demonstrating a direct parallel between indole lactam **8** and lactam **1**, the absorption bands associated with the formation of 1-pyridyliminium ion **10** (R = 3-chloro, 1679 cm^{–1}; R = 2-fluoro, 1652 cm^{–1}, Scheme 5) directly correlate to the IR absorption bands observed in the formation of 1-pyridyliminium ion **4b** (R = 3-chloro, 1679 cm^{–1}; R = 2-fluoro, 1659 cm^{–1}, Table 2). Additionally, the disappearance of the characteristic *O*-trifluoromethanesulfonyloxyiminium ion ¹⁹F NMR resonance (–71.4 ppm) of

sulfonyliminium ion **9** upon displacement with the base additive is consistent with formation of 1-pyridyliminium ion **10** and our earlier observations in formation of 1-pyridyliminium ion **4b**. Interestingly, the formation of 1-pyridyliminium ion **10** appears to increase the C13-electrophilicity and the rate of the subsequent spirocyclization to diiminium ion (\pm)-**11**. Specifically, when utilizing 3-cyanopyridine or 4-cyanopyridine as base additives, absorption bands corresponding to spirocyclization and formation of diiminium ion (\pm)-**11** (with 3-cyanopyridine: 1664 cm^{-1} and 1640 cm^{-1} ; with 4-cyanopyridine: 1664 cm^{-1} and 1635 cm^{-1}) are detected even at $-60\text{ }^\circ\text{C}$ by in situ IR monitoring.²⁸ The formation of dication **10** is also observed by NMR monitoring through the characteristic disappearance of the *O*-trifluoromethanesulfonyloxyiminium ion ^{19}F NMR resonance at -71.4 ppm, in addition to the maintained presence of the distinctive C2 ^1H NMR signal at 7.03 ppm that shifts to 10.02 ppm in diiminium ion (\pm)-**11**. All three intermediates **9**, **10**, and (\pm)-**11** revert back to indole lactam **8** upon exposure to water as observed by in situ NMR monitoring. Thus, prior to this informative in situ reaction monitoring investigation, evaluation of the reaction progress in our related mechanistic investigations was only possible through indirect and less accurate removal of cold aliquots from the reaction mixture followed by a reductive quench to prevent reversion to starting material.¹⁷

Finally, we conducted a series of experiments that focused on merging the knowledge gained from our in situ experiments, our prior findings, and isolable cyclization products. We first successfully accessed spiroindoline (\pm)-**12** in the absence of a base additive by sequential treatment of diiminium ion (\pm)-**11** with triethylsilane and lithium aluminum hydride in a 94% yield, compared to quantitative yield using 2-chloropyridine as a base additive.¹⁶ We were also able to selectively reduce the C2-iminium of diiminium ion (\pm)-**11**, by the use of triethylsilane alone, and isolated spiroindoline iminium ion (\pm)-**13** in 93% yield (Scheme 5, 1644 cm^{-1}). This iminium ion bears close resemblance to a fully characterized complex iminium ion from our earlier studies.^{17a} Specifically, characteristic values in the IR (1670 cm^{-1}), ^{19}F NMR (-78.6 ppm), and ^{13}C NMR (192.0 ppm) spectra of the hexacyclic iminium trifluoromethanesulfonate previously isolated are in accordance with the values we observed for spiroindoline iminium ion (\pm)-**13**. Importantly, the isolation and full characterization of spiroindoline iminium ion (\pm)-**13** is significant as it provides a bridge between final products such as tetracycle (\pm)-**12** and intermediates that are too fragile for isolation such as diiminium ion (\pm)-**11**. Indeed, the absorption band at 1644 cm^{-1} seen in the solution phase IR spectrum of spiroindoline iminium ion (\pm)-**13** is attributed to the C13-iminium ion functional grouping and is consistent with one of the two key IR absorption bands associated with the sensitive diiminium ion (\pm)-**11**.

Conclusions

We have described our mechanistic investigation of the electrophilic amide activation of α,α -disubstituted tertiary lactams using in situ FTIR, ^1H , ^{13}C , and ^{19}F NMR analysis, along with investigation of key intermediates relevant to our interrupted Bischler–Napieralski based synthetic strategy to the aspidosperma alkaloids. The treatment of a wide range of pyridines with trifluoromethanesulfonic anhydride was examined and characteristic IR absorption bands for the corresponding *N*-trifluoromethanesulfonylated pyridinium

trifluoromethanesulfonates were measured. The observed reversible formation of diiminium ether intermediates provided insight into competing reaction pathways available as a function of the steric environment of the amide substrate and stoichiometry of reagents. Importantly, we discovered that more hindered α -quaternary tertiary lactams require the use of non-nucleophilic pyridine additives in order to avoid deactivation via a competing desulfonylation reaction. The observed reactivity and stability of diiminium ion (\pm)-**11** and spiroindoline iminium ion (\pm)-**13** set the stage for further examination of potential late-stage functionalization and diversification of related synthetic intermediates, which will greatly impact new applications of our interrupted Bischler–Napieralski strategy toward the synthesis of the aspidosperma alkaloids. Additionally, we anticipate the notation of key IR absorption bands for reactive intermediates involved in amide activation using the Tf₂O–pyridine reagent combination, including *O*-trifluoromethanesulfonyloxyiminium ions, 1-pyridyliminium trifluoromethanesulfonate salts, diiminium ethers, and spiroindolines containing either one or two iminium ions, and the observed trends in reactivity using various pyridine additives will facilitate future mechanistic investigations and the development of related synthetic transformations.

EXPERIMENTAL SECTION

General Methods

All reactions were performed in oven-dried or flame-dried round-bottom flasks, modified Schlenk (Kjeldahl shape) flasks, NMR tubes or IR microcells.²⁹ The flasks were fitted with rubber septa, and reactions were conducted under a positive pressure of argon. Cannulae or gas-tight syringes with stainless steel needles were used to transfer air- or moisture-sensitive liquids. Flash column chromatography was performed as described by Still et al.³⁰ using granular silica gel (60-Å pore size, 40–63 μ m, 4–6% H₂O content) or non-activated alumina gel (80–325 mesh, chromatographic grade). Analytical thin layer chromatography (TLC) was performed using glass plates pre-coated with 0.25 mm 230–400 mesh silica gel impregnated with a fluorescent indicator (254 nm) or neutral alumina gel impregnated with a fluorescent indicator (254 nm). Thin layer chromatography plates were visualized by exposure to short wave ultraviolet light (254 nm) and irreversibly stained by treatment with an aqueous solution of ceric ammonium molybdate (CAM) or an aqueous solution of potassium permanganate (KMnO₄) followed by heating (~ 1 min) on a hot plate (~ 250 °C). Organic solutions were concentrated at 29–30 °C on rotary evaporators capable of achieving a minimum pressure of ~2 Torr. Proton (¹H), carbon (¹³C) and fluorine (¹⁹F) nuclear magnetic resonance spectra were recorded with 600 MHz, 500 MHz and 400 MHz spectrometers. Proton nuclear magnetic resonance (¹H NMR) spectra are reported in parts per million on the δ scale and are referenced from the residual protium in the NMR solvent. Chemical shifts are recorded in parts per million on the δ scale and are referenced from the residual protium in the NMR solvent (CHCl₃: δ 7.26, CHDCl₂: δ 5.32). Data are reported as follows: chemical shift [multiplicity (s = singlet, d = doublet, t = triplet, q = quartet, m = multiplet), coupling constant(s) in Hertz, integration, assignment]. Carbon-13 nuclear magnetic resonance spectra are recorded in parts per million on the δ scale and are referenced from the carbon signals of the solvent (CDCl₃: δ 77.16; CD₂Cl₂: δ 54.00). Data are reported as follows: chemical shift [multiplicity (s = singlet, d = doublet, t = triplet, q =

quartet, m = multiplet), coupling constant(s) in Hertz, assignment]. Fluorine-19 nuclear magnetic resonance spectra are recorded in parts per million on the δ scale and are referenced from the fluorine signals of trifluoromethanesulfonic anhydride ((CF₃SO₂)₂O δ -72.60). Data are reported as follows: chemical shift [multiplicity (s = singlet, d = doublet, t = triplet, q = quartet, m = multiplet), coupling constant(s) in Hertz, integration, assignment]. Infrared data (IR) were obtained with a FTIR and are reported as follows: [frequency of absorption (cm⁻¹), intensity of absorption (s = strong, m = medium, w = weak, br = broad)]. React-IR experiments were performed with a silicon probe. High-resolution mass spectrometric data (HRMS) were recorded on a FT-ICR-MS spectrometer using electrospray ionization (ESI) source or direct analysis in real time (DART) ionization source.

Formation and in situ analysis of *O*-trifluoromethanesulfonyloxyiminium ion **3a**

The iminium ion **3a** was observed using in situ IR analysis according to the following procedure: Trifluoromethanesulfonic anhydride (27.0 μ L, 161 μ mol, 1.20 equiv) was added via syringe to a solution of lactam **1a** (32.0 mg, 134 μ mol, 1 equiv) in dichloromethane (1.5 mL) at -78 °C. *O*-Trifluoromethanesulfonyloxyiminium ion **3a** was observed immediately. After 5 min, the reaction mixture was slowly warmed to 23 °C over the course of 1 h. No change in the IR spectrum of the reaction mixture was observed during the warming. IR (in CH₂Cl₂) cm⁻¹: 3057 (w), 2930 (m), 1692 (m), 1447 (br). The iminium ion **3a** was observed by NMR according to the following procedure: Trifluoromethanesulfonic anhydride (16.8 μ L, 100 μ mol, 1.20 equiv) was added via syringe to a solution of lactam **1a** (20.0 mg, 836 μ mol, 1 equiv) in dichloromethane-*d*₂ (750 μ L) at -78 °C. After 5 min, the reaction mixture was warmed to 0 °C. After 10 min, the ice bath was removed and the reaction mixture was allowed to warm to 23 °C. After 15 min at 23 °C, the reaction mixture was transferred to an NMR tube under an argon atmosphere via syringe. ¹H NMR (500 MHz, CD₂Cl₂, 20 °C): δ 4.02 (app-t, *J* = 5.6 Hz, 2H), 3.80 (app-t, *J* = 8.2 Hz, 2H), 3.27 (app-t, *J* = 6.1 Hz, 2H), 2.17–2.05 (m, 4H), 1.81–1.72 (m, 2H), 1.42–1.20 (m, 14H), 0.88 (t, *J* = 6.8 Hz, 3H). ¹³C NMR (125 MHz, CD₂Cl₂, 20 °C): δ 170.9, 118.7 (q, *J* = 323.8 Hz, OTf), 118.6 (q, *J* = 321.9 Hz, OTf), 56.6, 54.5, 32.4, 29.9, 29.8, 29.8, 29.7, 29.4, 27.1, 26.9, 23.2, 20.5, 18.3, 14.4. ¹⁹F NMR (282 MHz, CD₂Cl₂, 20 °C): δ -79.4 (OTf), -72.3 (COTf).

Formation and in situ analysis of *O*-trifluoromethanesulfonyloxyiminium ion **3b**

The iminium ion **3b** was observed using in situ IR analysis following the procedure for **3a** starting from **1b**. IR (in CH₂Cl₂) cm⁻¹: 3057 (s), 2930 (w), 1664 (m), 1462 (br). The iminium ion **3b** was observed by NMR following the procedure for **3a** starting from **1b**. ¹H NMR (500 MHz, CD₂Cl₂, 20 °C): δ 4.26 (app-t, *J* = 5.9 Hz, 2H), 3.99 (app-t, *J* = 8.7 Hz, 2H), 2.16–2.09 (m, 2H), 2.09–2.03 (m, 2H), 1.88–1.79 (m, 2H), 1.52 (s, 6H), 1.42–1.22 (m, 14H), 0.88 (t, *J* = 6.6 Hz, 3H). ¹³C NMR (125 MHz, CD₂Cl₂, 20 °C): δ 175.2, 121.4 (q, *J* = 320.9 Hz, OTf), 120.0 (q, *J* = 319.7 Hz, OTf), 58.5, 56.9, 41.2, 34.8, 32.4, 29.9, 29.8, 29.4, 27.7, 26.8, 26.0, 25.8, 23.1, 18.3, 14.4. ¹⁹F NMR (282 MHz, CD₂Cl₂, 20 °C): δ -71.1 (COTf), -79.7 (OTf).

Formation and in situ analysis of diiminium ether **6a**

The diiminium ion **6a** was observed using in situ IR analysis according to the following procedure: Trifluoromethanesulfonic anhydride (8.8 μL , 52 μmol , 0.50 equiv) was added via syringe to a solution of lactam **1a** (25.0 mg, 105 μmol , 1 equiv) in dichloromethane (1.5 mL) at $-78\text{ }^\circ\text{C}$. After 10 min, the reaction mixture was slowly warmed to $23\text{ }^\circ\text{C}$ over the course of 1 h. No change in the IR spectrum of the reaction mixture was observed during the warming. IR (in CH_2Cl_2) cm^{-1} : 2961 (s), 2930 (m), 1675 (m), 1478 (s). The diiminium ion **6a** was observed by NMR according to the following procedure: trifluoromethanesulfonic anhydride (7.0 μL , 42 μmol , 0.50 equiv) was added via syringe to a solution of lactam **1a** (20.0 mg, 83.6 μmol , 1 equiv) in dichloromethane- d_2 (750 μL) at $-78\text{ }^\circ\text{C}$. After 5 min, the reaction mixture was warmed to $0\text{ }^\circ\text{C}$. After 10 min, the reaction mixture was allowed to warm to $23\text{ }^\circ\text{C}$. The reaction mixture was transferred to an NMR tube under an argon atmosphere via syringe. ^1H NMR (400 MHz, CD_2Cl_2 , $25\text{ }^\circ\text{C}$): δ 4.00 (m, 4H), 3.94 (app-t, $J = 8.2\text{ Hz}$, 4H), 3.29 (app-t, $J = 5.5\text{ Hz}$, 4H), 2.12 (br-s, 8H), 1.84-1.75 (m, 4H), 1.43-1.17 (m, 8H), 0.88 (t, $J = 6.8\text{ Hz}$, 6H). ^{13}C NMR (100 MHz, CD_2Cl_2 , $25\text{ }^\circ\text{C}$): δ 172.0, 56.5, 54.1, 32.4, 30.5, 30.1, 29.9, 29.9, 29.8, 27.3, 27.1, 23.2, 20.5, 18.5, 14.4. ^{31}P NMR (376 MHz, CD_2Cl_2 , $25\text{ }^\circ\text{C}$): δ -79.6 (OTf).

Formation and in situ analysis of diiminium ether **6b**

The diiminium ion **6b** was observed using in situ IR analysis following the procedure for **6a** starting from **1b**. IR (in CH_2Cl_2) cm^{-1} : 3057 (m), 2930 (m), 1664 (m), 1462 (s).

Formation and in situ IR analysis of diiminium ether **7**

Formation of diiminium ion **7** via the addition of lactam **1b** to **3a** was observed using in situ IR analysis according to the following procedure: A cold solution of lactam **1b** (21.0 mg, 78.5 μmol , 1 equiv) in dichloromethane (500 μL , $-78\text{ }^\circ\text{C}$) was added to a solution of sulfonyliminium ion **3a** (78.5 μmol , 1 equiv) in dichloromethane (1.0 mL) at $-78\text{ }^\circ\text{C}$. After 5 min, the reaction mixture was slowly warmed to $23\text{ }^\circ\text{C}$ over the course of 1 h. IR (in CH_2Cl_2) cm^{-1} : 2930 (m), 2856 (w), 1675 (m), 1644 (m), 1467 (s). Formation of diiminium ion **7** via the addition of lactam **1a** to sulfonyliminium ion **3b** was observed using in situ IR analysis according to the following procedure: A cold solution of lactam **1a** (18.8 mg, 78.5 μmol , 1.00 equiv) in dichloromethane (500 μL , $-78\text{ }^\circ\text{C}$) was added to a solution of sulfonyliminium ion **3b** (78.5 μmol , 1 equiv) in dichloromethane (1.0 mL) at $-78\text{ }^\circ\text{C}$. After 5 min, the reaction mixture was slowly warmed to $23\text{ }^\circ\text{C}$ over the course of 1 h and then stirred at $23\text{ }^\circ\text{C}$ for 1 hour. IR (in CH_2Cl_2) cm^{-1} : 2932 (m), 2859 (w), 1675 (m), 1644 (m), 1484 (s).

Formation and in situ analysis of *N*-(trifluoromethylsulfonyl)pyridinium trifluoromethanesulfonates **5** (Table 1)

In situ IR monitoring of the addition of trifluoromethanesulfonic anhydride (42.2 μL , 251 μmol , 1 equiv) to a solution of pyridine derivative **2** (251 μmol , 1 equiv) in dichloromethane (1.5 mL) at $-78\text{ }^\circ\text{C}$ under argon resulted in the formation of the expected *N*-(trifluoromethylsulfonyl)pyridinium trifluoromethanesulfonate **5**. After 5 min, the reaction

mixture was slowly warmed to 23 °C over the course of 1 h. Scans were collected at 30-second intervals.

Formation and in situ IR analysis of 1-pyridyliminium ions **4** (Table 2)

Trifluoromethanesulfonic anhydride (18.8 μL , 112 μmol , 1.20 equiv) was added via syringe to a solution of lactam **1** (93.9 μmol , 1 equiv) and pyridine additive (112 μmol , 1.20 equiv) in dichloromethane (1.5 mL) at -78 °C. After 5 min, the reaction mixture was slowly warmed to 23 °C over the course of 1 h. The representative IR spectrum for formation of pyridinium ion **4b** is illustrative: 1687 (m), 1629 (m), 1486 (m), 1428 (s).

Representative formation and in situ NMR analysis of 1-pyridyliminium ion **4b** (R=3-Cl, Table 2, entry 5)

Trifluoromethanesulfonic anhydride (28.0 μL , 166 μmol , 1.70 equiv) was added via syringe to dichloromethane- d_2 (0.3 mL) in an NMR tube under argon and subsequently cooled to -78 °C. A solution of lactam **1b** (26.0 mg, 97.9 μmol , 1 equiv) and 3-chloropyridine (15.8 μL , 164 μmol , 1.70 equiv) in dichloromethane- d_2 (450 μL) at -78 °C was added to the cooled trifluoromethanesulfonic anhydride solution via syringe. After 5 min, the reaction mixture was warmed to 0 °C. After 10 min, the reaction mixture was allowed to warm to 23 °C and sonicated for 15 min. ^1H NMR (400 MHz, CD_2Cl_2 , 25 °C)³²: δ 9.71 (s, 1H), 9.55 (d, J = 6.9 Hz, 1H), 8.98 (d, J = 8.5 Hz, 1H), 8.56 (dd, J = 6.4, 8.5 Hz, 1H), 4.41 (app-t, J = 5.5 Hz, 2H), 3.64–3.51 (m, 2H), 2.39–2.28 (m, 2H), 2.23–2.14 (m, 2H), 1.96–1.86 (m, 2H), 1.49 (s, 3H), 1.48 (s, 3H), 1.32–1.11 (m, 14H), 0.85 (t, J = 6.9 Hz, 3H). ^{13}C NMR (100 MHz, CDCl_3 , 25 °C): δ 175.5, 152.6, 142.7, 142.5, 139.3, 131.3, 61.8, 58.0, 42.6, 33.0, 32.4, 29.9, 29.7, 29.7, 29.2, 27.1, 27.0, 26.8, 26.6, 23.2, 18.0, 14.4.³¹ ^{19}F NMR (376 MHz, CD_2Cl_2 , 25 °C): δ -79.8 (OTf).

Formation of pyridinium ion **5** from *O*-trifluoromethanesulfonyloximinium trifluoromethanesulfonate **3b**

Pyridine (21.1 μL , 262 μmol , 2.00 equiv) was added via syringe to a solution of sulfonyliminium ion **3b** (131 μmol , 1 equiv) in dichloromethane (1.5 mL) at -78 °C. Immediate reversion of sulfonyliminium ion **3b** to lactam **1b** and formation of *N*-(trifluoromethylsulfonyl)pyridinium trifluoromethanesulfonate **5** was observed. The reaction was monitored for 1.5 h and no change was observed. IR (in CH_2Cl_2) cm^{-1} : 1687 (s), $\text{C}_5\text{H}_5\text{N}^+-\text{SO}_2\text{CF}_3$, 1625 (s), 1582 (s), 1482 (br), 1432 (br).

Formation and in situ IR and NMR analysis of tetracyclic iminium ion (\pm)-**11**

Tetracyclic iminium ion (\pm)-**11** was observed using in situ IR analysis according to the following procedure: Trifluoromethanesulfonic anhydride (21.3 μL , 127 μmol , 1.20 equiv) was added via syringe to a solution of lactam **8** (30.0 mg, 105 μmol , 1 equiv) in dichloromethane (1.5 mL) at -78 °C. After 5 min, the reaction mixture was slowly warmed to 23 °C over the course of 1 h. IR (in CH_2Cl_2) cm^{-1} : 1664 (m), 1644 (m), 1613 (w), 1586 (s). Tetracyclic iminium ion (\pm)-**11** was observed using in situ NMR according to the following procedure: Trifluoromethanesulfonic anhydride (30.1 μL , 179 μmol , 1.70 equiv) was added via syringe to dichloromethane- d_2 (0.3 mL) in an NMR tube equipped with a

rubber septum under argon and subsequently cooled to $-78\text{ }^{\circ}\text{C}$. A solution of lactam **8** (30.0 mg, 105 μmol , 1 equiv) in dichloromethane- d_2 (450 μL) at $-78\text{ }^{\circ}\text{C}$ was added to the cooled Tf_2O solution. The NMR tube was immediately transferred to a cooled NMR probe at $-80\text{ }^{\circ}\text{C}$. The reaction mixture was warmed at a rate of $1\text{ }^{\circ}\text{C}/\text{min}$, affording the data illustrated in Figure 1 for *O*-trifluoromethanesulfonyloximinium trifluoromethanesulfonate **9**. ^1H NMR (400 MHz, CD_2Cl_2 , $-40\text{ }^{\circ}\text{C}$): δ 7.49 (d, $J = 8.0\text{ Hz}$, 1H), 7.34 (d, $J = 8.1\text{ Hz}$, 1H), 7.22 (app-t, $J = 7.7\text{ Hz}$, 1H), 7.11 (app-t, $J = 7.7\text{ Hz}$, 1H), 7.03 (s, 1H), 4.22 (t, $J = 6.9\text{ Hz}$, 2H), 3.97 (br-s, 2H) 3.72 (s, 3H), 3.27 (t, $J = 6.9\text{ Hz}$, 2H), 1.81 (s, 4H), 1.31 (s, 6H). ^{13}C NMR (100 MHz, CD_2Cl_2 , $-40\text{ }^{\circ}\text{C}$): δ 174.6, 136.6, 127.8, 126.7, 122.1, 119.5, 117.9, 118.1 (q, $J = 322.2\text{ Hz}$, OTf), 114.7 (q, $J = 333.9\text{ Hz}$, OTf), 110.0, 106.7, 58.6, 57.1, 40.5, 33.8, 33.0, 24.9, 23.2, 17.5. ^{19}F NMR (376 MHz, CD_2Cl_2 , $-40\text{ }^{\circ}\text{C}$): δ -71.4 (COTf), -79.9 (OTf). Tetracyclic diiminium ion (\pm)-**11**: ^1H NMR (400 MHz, CD_2Cl_2 , $0\text{ }^{\circ}\text{C}$): δ 10.02 (s, 1H), 8.27 (d, $J = 6.5\text{ Hz}$, 1H), 7.89–7.84 (m, 1H), 7.85–7.77 (m, 2H), 4.76–4.61 (m, 2H), 4.33 (s, 1H), 4.24 (d, $J = 12.7\text{ Hz}$, 1H), 3.98–3.87 (m, 1H), 3.19–3.07 (m, 1H), 3.07–2.97 (m, 1H), 2.20 (br-s, 1H), 2.09–1.99 (m, 1H), 1.85 (t, $J = 12.7\text{ Hz}$, 1H), 1.63–1.55 (m, 1H), 1.05 (s, 1H), 0.82 (s, 1H). ^{13}C NMR (125 MHz, CD_2Cl_2 , $0\text{ }^{\circ}\text{C}$): δ 187.9, 176.2, 151.6, 142.9, 135.9, 133.4, 132.8, 117.6, 70.3, 61.6, 52.5, 40.4, 39.2, 34.0, 30.4, 28.6, 24.6, 17.9.³¹ ^{19}F NMR (376 MHz, CD_2Cl_2 , $0\text{ }^{\circ}\text{C}$): δ -79.6 (OTf).

Spiroindoline (\pm)-**12**¹⁶

Trifluoromethanesulfonic anhydride (12.1 μL , 71.8 μmol , 1.20 equiv) was added via syringe to a solution of lactam **8** (17.0 mg, 59.8 μmol , 1 equiv) and 2-chloropyridine (12.4 μL , 122 μmol , 2.20 equiv) in dichloromethane (750 μL) at $-78\text{ }^{\circ}\text{C}$. After 5 min, the reaction mixture was warmed to $0\text{ }^{\circ}\text{C}$. After 10 min, the reaction mixture was allowed to warm to $23\text{ }^{\circ}\text{C}$. After 20 min, triethylsilane (28.6 μL , 179 μmol , 3.00 equiv) was added via syringe. After 2 h, the reaction mixture was cooled to $0\text{ }^{\circ}\text{C}$, and THF (750 μL) was added via syringe. After 30 seconds, lithium aluminum hydride (9.10 mg, 240 μmol , 4.00 equiv) was added as a solid under argon atmosphere. After 10 min at $0\text{ }^{\circ}\text{C}$, a solution of potassium sodium tartrate was added to quench the unreacted aluminum hydride salts. The reaction mixture was allowed to warm to $23\text{ }^{\circ}\text{C}$. The layers were separated and the aqueous layer was extracted with dichloromethane ($3 \times 5\text{ mL}$). The combined organic extracts were washed with saturated aqueous sodium chloride solution (10 mL), were dried over anhydrous sodium sulfate, were filtered, and were concentrated under reduced pressure. The resulting residue was purified by flash column chromatography on alumina gel (eluent: $0 \rightarrow 10\%$ ethyl acetate in hexanes) to give spiroindoline (\pm)-**12** (16.0 mg, 98.9%) as an off-white powder. When the same procedure was executed without base, the desired product was obtained in 94.0% isolated yield. When the same procedure was executed without triethylsilane, the desired product was obtained in 73.6% isolated yield. The analytical data for the isolated compound in each case was consistent with our previously reported data.¹⁶

Spiroindoline iminium ion (\pm)-**13**

Trifluoromethanesulfonic anhydride (20.9 μL , 125 μmol , 1.20 equiv) was added via syringe to a solution of lactam **8** (29.5 mg, 104 μmol , 1 equiv) in dichloromethane (1.0 mL) at $-78\text{ }^{\circ}\text{C}$. After 5 min, the reaction mixture was warmed to $0\text{ }^{\circ}\text{C}$. After 10 min, the reaction mixture was allowed to warm to $23\text{ }^{\circ}\text{C}$. After 20 min, triethylsilane (166 μL , 1.04 mmol,

10.0 equiv) was added via syringe. After 2 h, pyridine (83.7 μL , 1.04 mol, 10.0 equiv) was added via syringe. After 14 h, the reaction mixture was concentrated under reduced pressure. The resulting residue was purified by flash column chromatography on alumina gel (eluent: 0 \rightarrow 100% acetone in hexanes) to give spiroindoline iminium ion (\pm)-**13** (40.4 mg, 93.0%) as a pale yellow oil. ^1H NMR (500 MHz, CDCl_3 , 20 $^\circ\text{C}$): δ 7.22 (app-dt, $J = 1.2, 7.8$ Hz, 1H), 7.04 (d, $J = 7.5$ Hz, 1H), 6.71 (app-t, $J = 7.5$ Hz, 1H), 6.55 (d, $J = 7.9$ Hz, 1H), 4.43 (ddd, $J = 6.4, 8.4, 14.4$ Hz, 1H), 4.23–4.16 (m, 1H), 4.19 (d, $J = 11.3$ Hz, 2H), 4.16–4.23 (m, 1H), 3.88 (m, 1H), 3.39 (d, $J = 11.3$ Hz, 1H), 2.82 (s, 3H), 2.73–2.62 (m, 1H), 2.62–2.54 (m, 1H), 2.16–2.07 (m, 1H), 2.07–1.96 (m, 1H), 1.89 (ddd, $J = 3.4, 10.0, 13.3$ Hz, 1H), 1.58 (ddd, $J = 3.1, 7.8, 13.6$ Hz, 1H), 1.50 (s, 3H), 0.89 (s, 3H). ^{13}C NMR (125 MHz, CDCl_3 , 20 $^\circ\text{C}$): δ 193.7, 152.7, 130.9, 129.0, 124.7, 121.0 (q, $J = 320.4$ Hz, OTf), 118.6, 108.4, 65.0, 62.9, 58.4, 50.6, 38.4, 36.5, 35.2, 35.1, 28.2, 26.0, 17.5. ^{19}F NMR (282 MHz, CDCl_3 , 20 $^\circ\text{C}$): δ -79.1. FTIR (thin film) cm^{-1} : 3567 (w), 3056 (m), 2957 (s), 2873 (s), 1652 (s), 1605 (s), 1497 (s), 1031 (s), 755 (s), 638 (s). HRMS (ESI) (m/z): calc'd for $\text{C}_{18}\text{H}_{25}\text{N}_2^+$ [M] $^+$: 269.2012, found: 269.2020. M.p.: 110–112 $^\circ\text{C}$. TLC (Al_2O_3 , 50% acetone in hexanes), R_f: 0.45 (UV, CAM).

Supplementary Material

Refer to Web version on PubMed Central for supplementary material.

ACKNOWLEDGMENTS

We are grateful for financial support by NIH-NIGMS (GM074825) and Amgen. K. L. W. acknowledges a National Science Foundation graduate fellowship. M. Mewald thanks the German Academic Exchange Service (DAAD) for a postdoctoral fellowship.

REFERENCES

1. For reviews, see: Stang PJ, Hanack LR, Subramanian LR. *Synthesis*. 1982:85. Baraznenok IL, Nenajdenko VG, Balenkova ES. *Tetrahedron*. 2000; 56:3077.
2. Myers AG, Tom NJ, Fraley ME, Cohen SB, Madar DJ. *J. Am. Chem. Soc.* 1997; 119:6072.
3. Garcia BA, Gin DY. *J. Am. Chem. Soc.* 2000; 122:4269.
4. (a) Movassaghi M, Hill MD. *J. Am. Chem. Soc.* 2006; 128:4592. [PubMed: 16594694] (b) Movassaghi M, Hill MD, Ahmad OK. *J. Am. Chem. Soc.* 2007; 129:10096. [PubMed: 17663557]
5. Movassaghi M, Hill MD. *J. Am. Chem. Soc.* 2006; 128:14254. [PubMed: 17076488]
6. Ahmad OK, Hill MD, Movassaghi M. *J. Org. Chem.* 2009; 74:8460. [PubMed: 19810691]
7. Movassaghi M, Hill MD. *Org. Synth.* 2008; 85:88.
8. Movassaghi M, Hill MD. *Org. Lett.* 2008; 10:3485. [PubMed: 18642832]
9. Medley JW, Movassaghi M. *J. Org. Chem.* 2009; 74:1341. [PubMed: 19113815]
10. For other applications of the TiF_2O –2-chloropyridine reagent combination, see: Cui S-L, Wang J, Wang Y-G. *J. Am. Chem. Soc.* 2008; 130:13526. [PubMed: 18798615] Barbe G, Pelletier G, Charette AB. *Org. Lett.* 2009; 11:3398. [PubMed: 19719187]
11. (a) Barbe G, Charette AB. *J. Am. Chem. Soc.* 2008; 130:18. [PubMed: 18076177] (b) Xiang S-H, Xu J, Yuan H-Q, Huang P-Q. *Synlett*. 2010:1829. (c) Pelletier G, Bechara WS, Charette AB. *J. Am. Chem. Soc.* 2010; 132:12817. [PubMed: 20735125]
12. (a) Xiao K-J, Luo J-M, Ye K-Y, Wang Y, Huang P-Q. *Angew. Chem. Int. Ed.* 2010; 49:3037. (b) Xiao K-J, Wang Y, Ye K-Y, Huang P-Q. *Chem.–Eur. J.* 2010; 16:12792. [PubMed: 20938943] (c) Xiao K-J, Wang A-E, Huang P-Q. *Angew. Chem. Int. Ed.* 2012; 51:8314.
13. Peng B, Geerdink D, Fares C, Maulide N. *Angew. Chem. Int. Ed.* 2014; 53:5462.

14. Bechara WS, Pelletier G, Charette AB. *Nature Chem.* 2012; 4:228. [PubMed: 22354438]
15. For related applications of Tf₂O, see: Valerio V, Petkova D, Madelaine C, Maulide N. *Chem.–Eur. J.* 2013; 19:2606. [PubMed: 23307662] Pace V, Castoldi L, Holzer W. *Chem. Commun.* 2013; 49:8383. Peng B, Geerdink D, Maulide N. *J. Am. Chem. Soc.* 2013; 135:14968. [PubMed: 24079481] Peng B, Geerdink D, Fares C, Maulide N. *Angew. Chem. Int. Ed.* 2014; 53:8718. Pace V, Castoldi L, Mamuye AD, Holzer W. *Synthesis.* 2014:2897.
16. Medley JW, Movassaghi M. *Org. Lett.* 2013; 15:3614. [PubMed: 23829389]
17. (a) Medley JW, Movassaghi M. *Angew. Chem. Int. Ed.* 2012; 51:4572.(b) Mewald M, Medley JW, Movassaghi M. *Angew. Chem. Int. Ed.* 2014; 53:11634.
18. (a) Charette AB, Grenon M. *Can. J. Chem.* 2001; 79:1694.(b) Charette AB, Mathieu S, Martel J. *Org. Lett.* 2005; 7:5401. [PubMed: 16288516]
19. For a report on alkoxy carbonyl-substituted 3-trifloxypyrone iminium salts and iminium substituted 2,3-butenolides with NMR characterization, see: Nikolai J, Maas G. *Synthesis.* 2003:2679.
20. For a report on the investigation of Tf₂O-mediated activation of valerolactam, see: Kuhnert N, Clemens I, Walsh R. *Org. Biomol. Chem.* 2005; 3:1694. [PubMed: 15858652]
21. While there are other representative absorption bands for the key substrates observed by in situ IR, we selected to focus on the range between 1600–1700 cm⁻¹ due to the absence of other peaks in this region that could interfere with our assignments. Additionally, this range was consistent with preliminary calculations (EDF2/631G* and SM8) suggesting the occurrence of key absorption bands for possible intermediates.
22. Stang PJ, Maas G, Fisk TE. *J. Am. Chem. Soc.* 1980; 102:6361.
23. For examples of sensitive intermediates formed during electrophilic activation with Tf₂O, such as diiminium ion ethers, see: Singer B, Maas G. *Chem. Ber.* 1987; 120:485. Alder RW, Butts CP, Orpen AG. *J. Am. Chem. Soc.* 1998; 120:11526. For diamidinium ion and diguanidinium ion ethers, see: Stang PJ, Maas G, Smith DL, McCloskey JA. *J. Am. Chem. Soc.* 1981; 103:4837. Gramstad T, Husebye S, Saebø J. *Tetrahedron Lett.* 1983; 24:3919. Maas G, Brückmann R, Feith B. *J. Heterocyclic Chem.* 1985; 22:907. Feith B, Weber H-M, Maas G. *Chem. Ber.* 1986; 119:3276. Kunkel H, Maas G. *Eur. J. Org. Chem.* 2007:3746.
24. Notably, the same absorption bands are observed for diiminium ethers **6a** and **6b**. However, the data supports the formation of the mixed diiminium ethers because no formation of *O*-trifluoromethanesulfonyloxyiminium trifluoromethanesulfonate **3b**, required in the formation of **6b**, is detected in this reaction.
25. (a) Binkley RW, Ambrose MG. *J. Org. Chem.* 1983; 48:1776.(b) Netscher T, Bohrer P. *Tetrahedron Lett.* 1996; 37:8359.
26. Bull JA, Mousseau JJ, Pelletier G, Charette A. *Chem. Rev.* 2012; 112:2642. [PubMed: 22352938]
27. Electron rich pyridines including 3-methoxypyridine and 4-dimethylaminopyridine, resulted in the formation of stabilized *N*-sulfonyl pyridinium ions **5** that did not allow for activation of either lactam **1a** or **1b** even at 23 °C.
28. In the presence of pyridine additives, the IR absorption bands for diiminium ion (±)-**11** shift very slightly compared to those seen in the absence of additives. For example, the characteristic absorption bands for diiminium ion (±)-**11** at 1664 cm⁻¹ and 1644 cm⁻¹ in the absence of 3-cyanopyridine shift to absorption bands at 1664 cm⁻¹ and 1640 cm⁻¹, respectively, in the presence of 3-cyanopyridine. This is observed whether the base additive is present during or after amide activation.
29. Kelly TR, Silva RA, Finkenbeiner G. *Tetrahedron Lett.* 2000; 41:9651.
30. Still WC, Kahn M, Mitra A. *J. Org. Chem.* 1978; 43:2923.
31. The sensitive nature of this product did not permit extended data collection for unambiguous assignment of the trifluoromethyl ¹³C-resonances as in other cases described in this study.
32. The minor broad peaks present in the ¹H NMR spectrum between 8.6–8.9 ppm correspond to the 3-chloro-*N*-sulfonyl pyridinium ion due to the excess 3-chloropyridine and Tf₂O used in the NMR experiment.

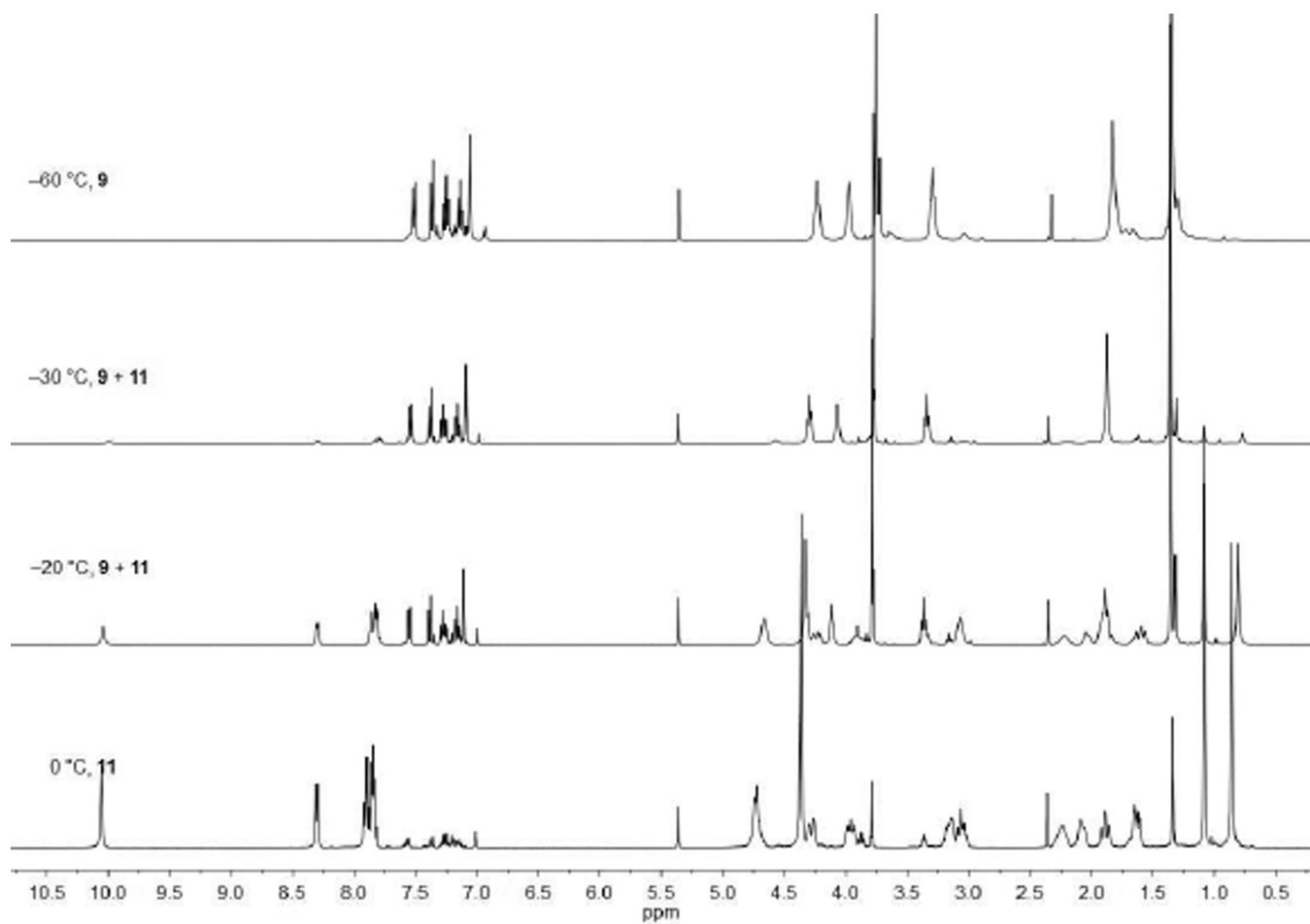
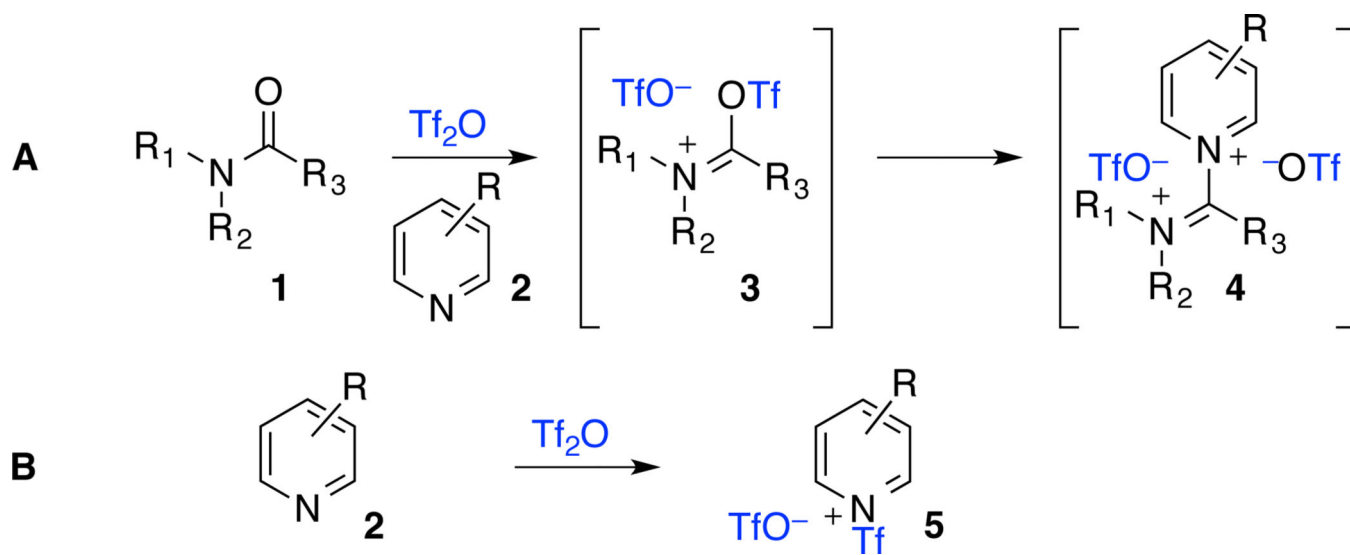
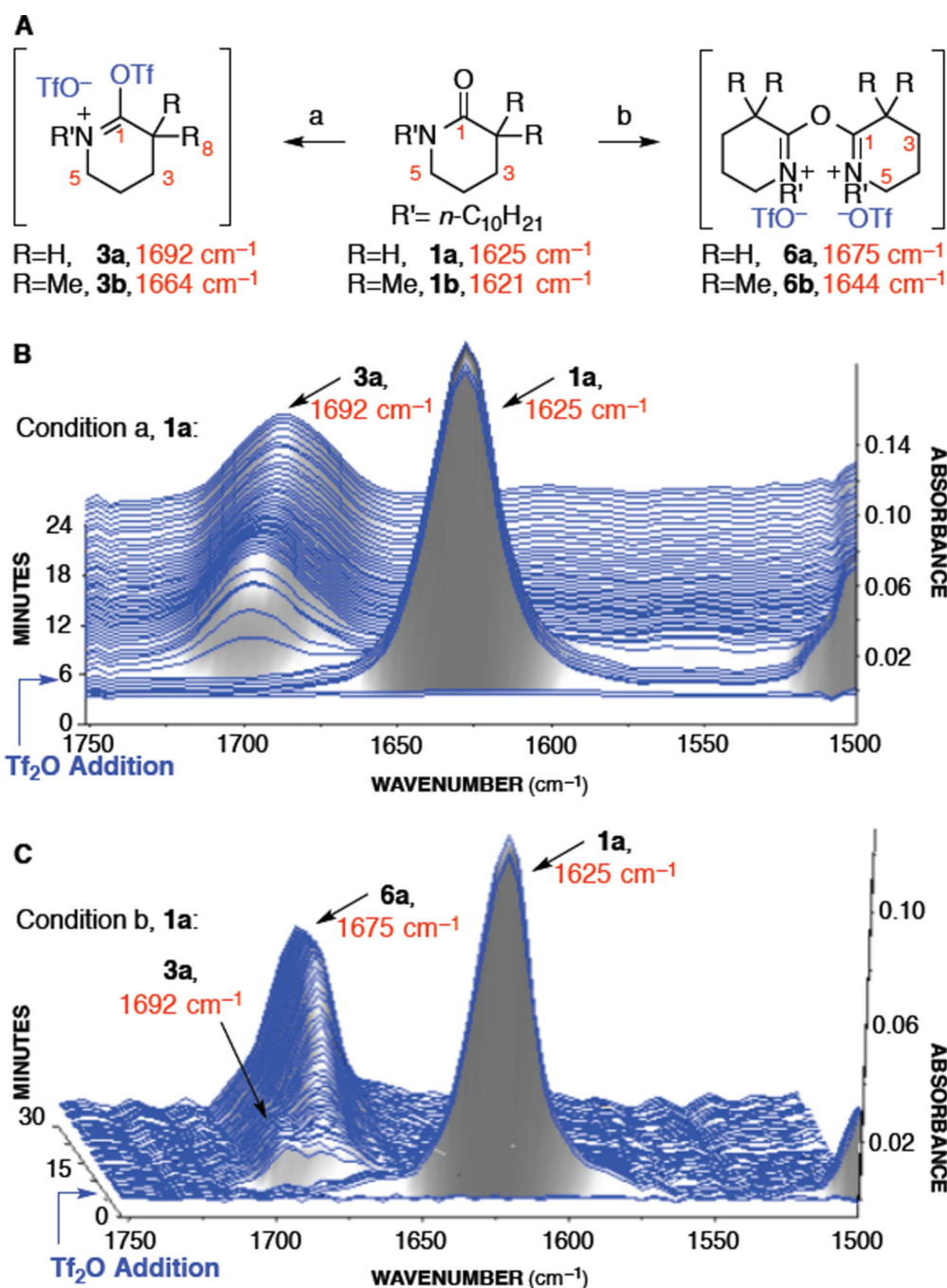


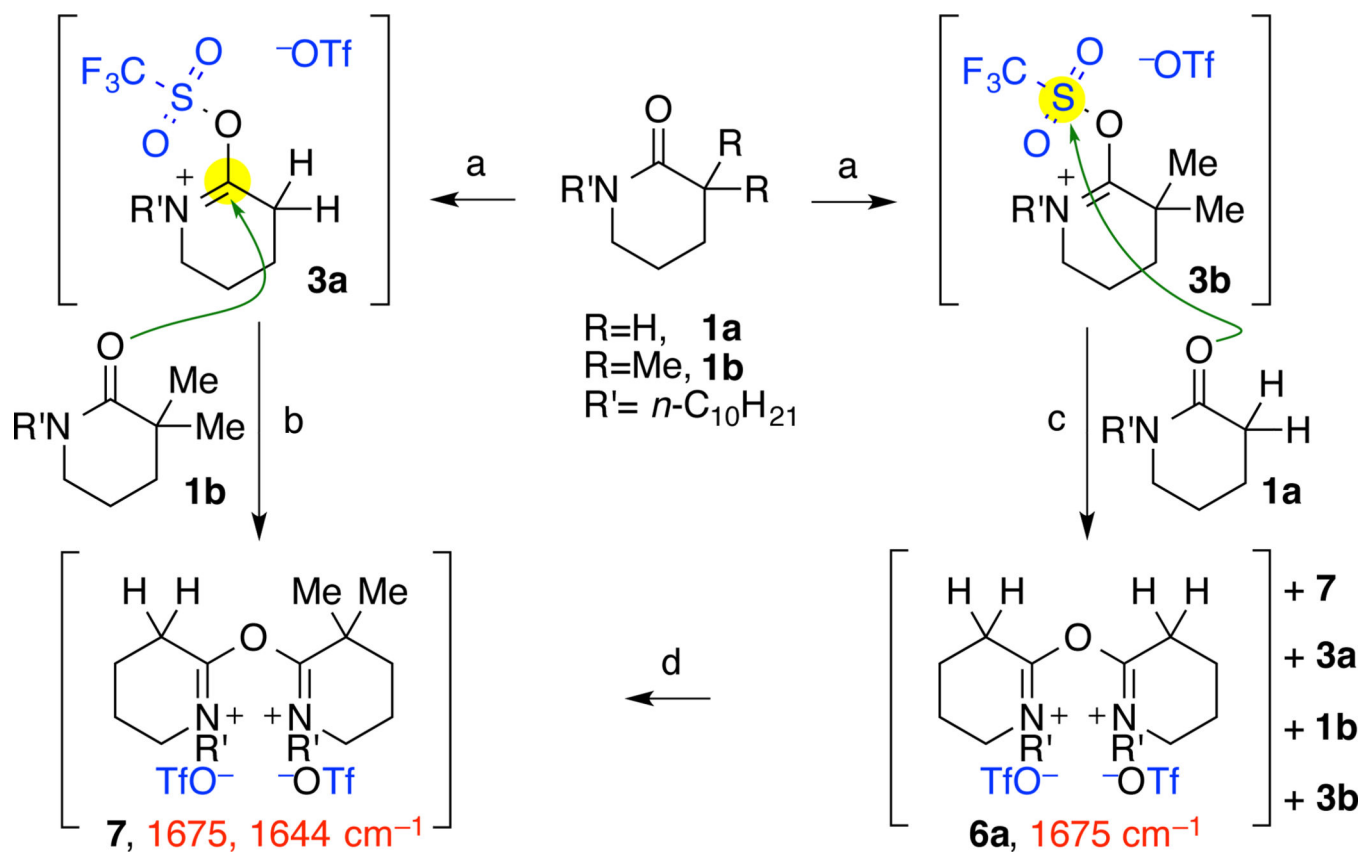
Figure 1.
Low Temperature Activation of Lactam **8** and Observation of Diiminium Ion (\pm)-**11** by ¹H NMR.

**Scheme 1.**

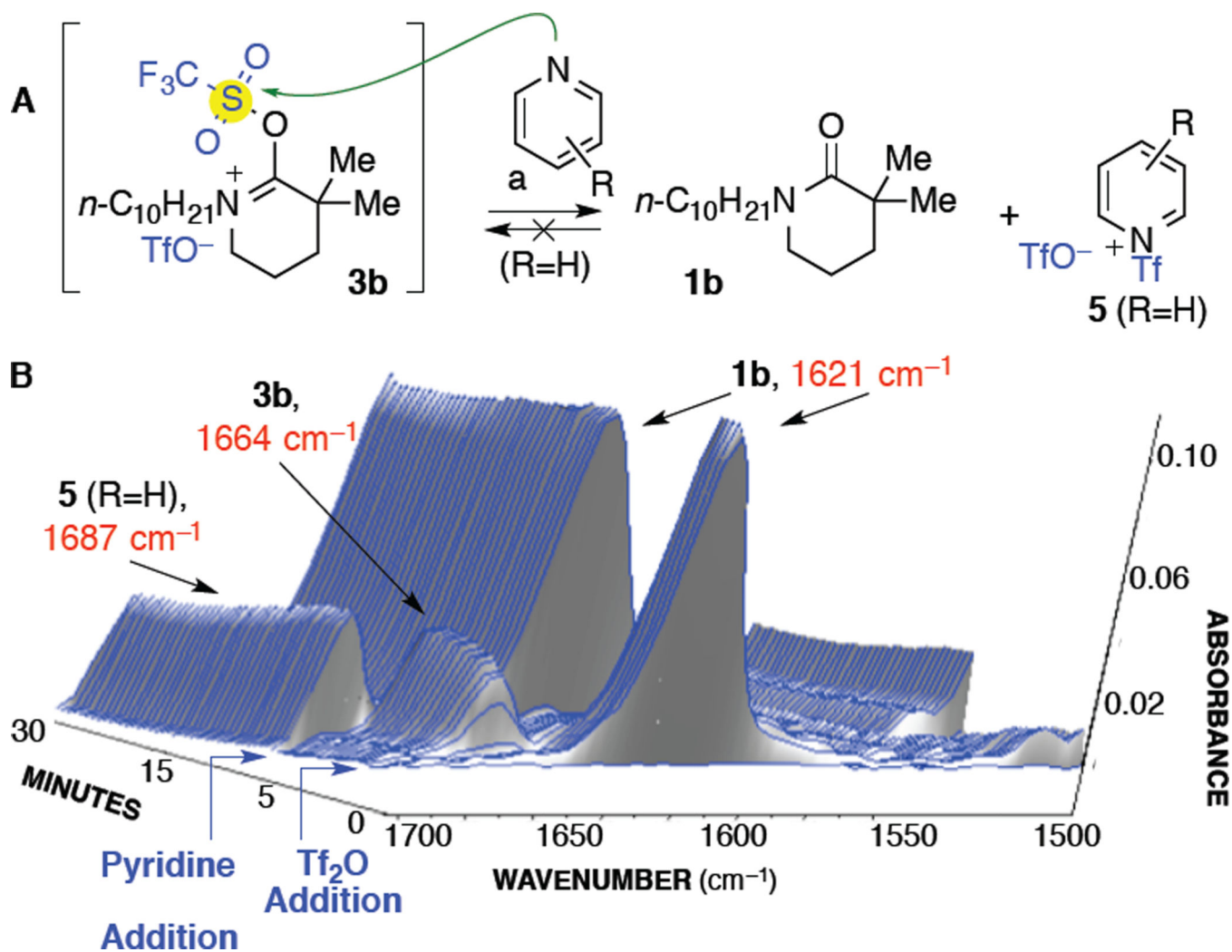
A. Electrophilic Tertiary Amide Activation with Tf₂O. **B.** *N*-Sulfonylation of Pyridines.

**Scheme 2.**

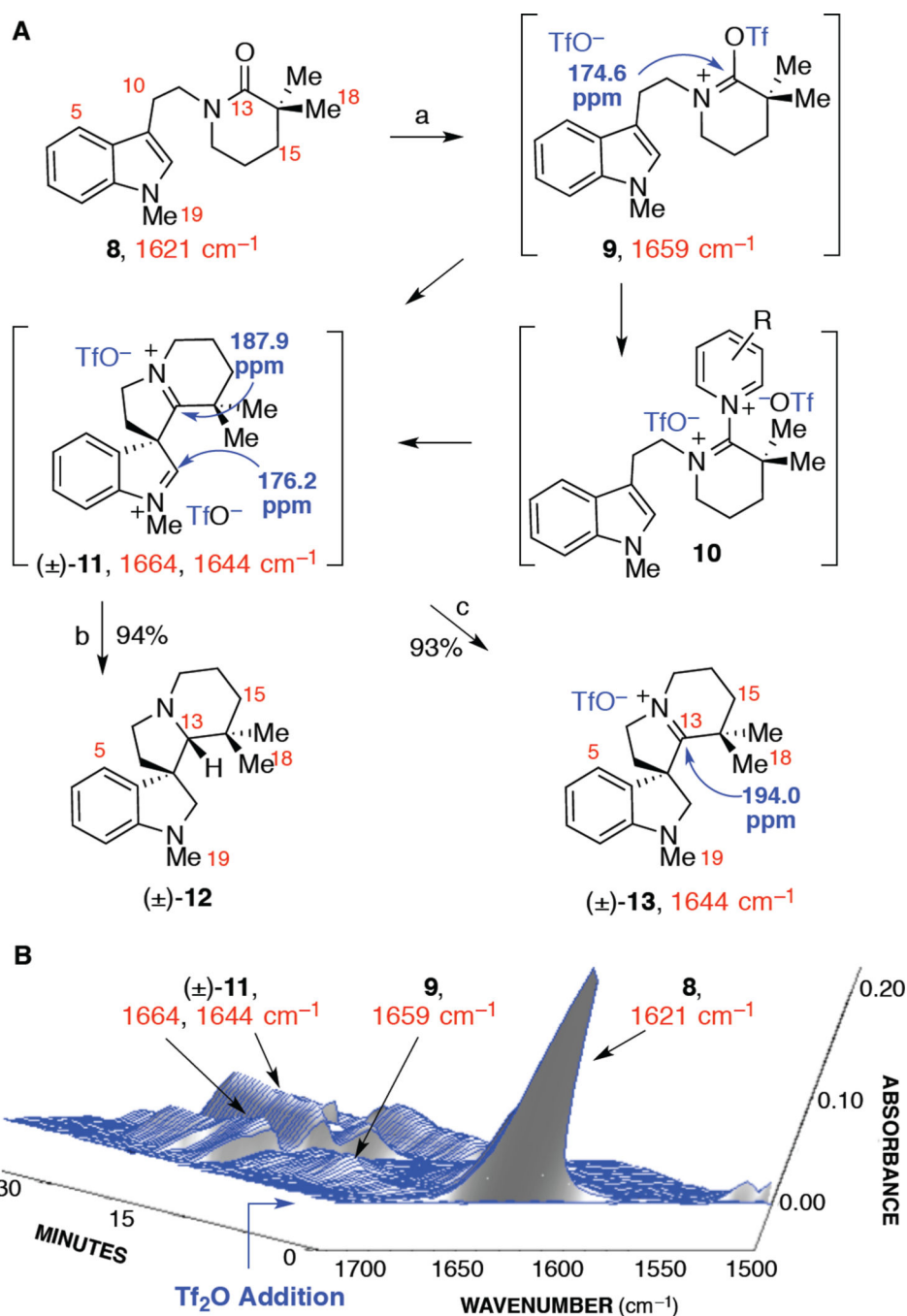
Electrophilic Activation of Lactams. **A**. Conversion of lactams **1** to sulfonyl iminium ions **3** and diiminium ethers **6**. Conditions: (a) Tf_2O (1.0 equiv), CH_2Cl_2 , -78°C . (b) Tf_2O (0.5 equiv), CH_2Cl_2 , -78°C (**6a**) or $-78 \rightarrow 23^\circ\text{C}$ (**6b**). **B**. Representative conversion of lactam **1a** to sulfonyl iminium ion **3a** monitored by in situ IR. **C**. Representative conversion of lactam **1a** to diiminium ether **6a** monitored by in situ IR. Key IR absorption bands are reported in wavenumber and shown in red.

**Scheme 3.**

Formation and Equilibration of Diiminium Ethers. Conditions: (a) Tf_2O (1.0 equiv), CH_2Cl_2 , $-78 \rightarrow 23 \text{ }^\circ\text{C}$. (b) $\mathbf{1b}$ (1.0 equiv); $-78 \rightarrow 23 \text{ }^\circ\text{C}$. (c) $\mathbf{1a}$ (1.0 equiv); $-78 \rightarrow 23 \text{ }^\circ\text{C}$. (d) 30 min, $23 \text{ }^\circ\text{C}$. Key IR absorption bands are reported in wavenumber and shown in red.



Scheme 4. Deactivation in the Presence of Pyridine. **A.** Conditions: (a) pyridine (2 equiv), CH_2Cl_2 , $-78^\circ\text{C} \rightarrow 23^\circ\text{C}$. **B.** Activation of lactam **1b** in the form of sulfonil iminium ion **3b**, followed by its deactivation upon treatment with pyridine. Key IR absorption bands are reported in wavenumber and shown in red.

**Scheme 5.**

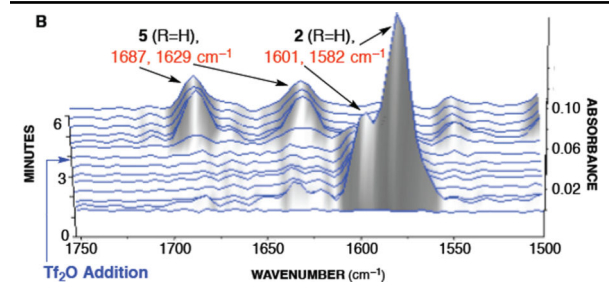
Direct Observation and Study of Spirocyclic Diiminium Ion (\pm)-**11**. **A**. Conditions: (a) Tf_2O (1.2 equiv), CH_2Cl_2 or CD_2Cl_2 , $-78 \rightarrow 23$ $^\circ\text{C}$. (b) Et_3SiH , 23 $^\circ\text{C}$; LiAlH_4 , THF, $0 \rightarrow 23$ $^\circ\text{C}$. (c) Et_3SiH , 23 $^\circ\text{C}$; pyridine. **B**. Conversion of lactam **8** to tetracyclic bisiminium ion (\pm)-**11** monitored by in situ IR. Key ^{13}C NMR resonances (blue) and IR absorption bands (red) are noted.

Table 1

N-Sulfonylation of Pyridine Derivatives.

A

Entry	R	2 (cm ⁻¹)	5 (cm ⁻¹)
1	H	1601, 1582	1687, 1629
2	2-Cl	1578	-
3	2-F	1621	1636
4	3-Cl	1571	1598
5	3-Br	1575	1675
6	3-CN	1587	1621
7	3-C(O)OEt	1718, 1581	1741, 1640
8	2-C(O)OEt	1718, 1590	1752, 1664
9	4-CN	1594	1629
10	3-OMe	1671	1690, 1653
11	4-NMe ₂	1601	1648, 1594



A. Key IR absorption bands are reported in wavenumber.

B. Representative formation of *N*-(trifluoromethylsulfonyl)pyridinium trifluoromethanesulfonate **5** (R=H) monitored by in situ IR.

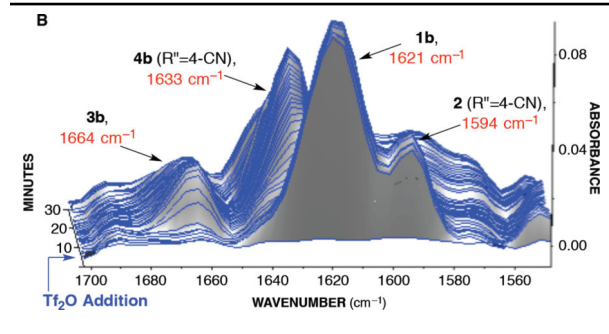
Table 2

Formation of 1-Pyridyliminium Ion Derivatives **4**.

A

Reaction scheme showing the formation of 1-pyridyliminium ion derivatives **4** from lactams **1a** and **1b** (where $R' = n\text{-C}_{10}\text{H}_{21}$) using Tf_2O and various additives. The reaction proceeds through intermediates **3a** and **3b** to form the final products **4a** and **4b**.

Entry	Lactam	Additive	Temp. ($^{\circ}\text{C}$) ^b	4 (cm^{-1}) ^c
1	1a	2-ClPyr	-78	1682
2	1a	3-BrPyr	-78	1660
3	1a	pyridine	-78	1679
4	1b	2-ClPyr	-60	1617
5	1b	2-FPyr	23	1659
6	1b	3-ClPyr	-78	1679
7 ^d	1b	3-CNPyr	-78	1679
8 ^d	1b	4-CNPyr	-78	1633



A. Key IR absorption bands are reported in wavenumber.

(a) Conditions: Tf_2O (1.2 equiv), additive (1.2 equiv), $-78\text{ }^{\circ}\text{C} \rightarrow 23\text{ }^{\circ}\text{C}$.

(b) The temperature noted corresponds to the temperature at which **4** was first detected.

(c) A key IR absorption band (wavenumber) of the corresponding 1-pyridyliminium ion **4**.

(d) The addition of lactam last resulted in the same outcome.

B. Representative formation of 1-pyridyliminium ion **4b** ($R'' = 4\text{-CN}$) monitored by in situ IR.